CRISPR-Edited DPSCs, Constitutively Expressing BDNF Enhance Dentin Regeneration in Injured Teeth

Ji Hyun Kim[1#], Muhammad Irfan[1#], Sreelekshmi Sreekumar[1], Stephanie Kim[1], Atsawasuwan Phimon[2], Seung Chung[1*]

[1]Department of Oral Biology, College of Dentistry, University of Illinois Chicago, Chicago 60612, IL, USA

[2]Department of Orthodontics, College of Dentistry, University of Illinois Chicago, Chicago 60612, IL, USA

[#]Co-first authors

*Correspondence to: Dr. S. Chung, Department of Oral Biology, College of Dentistry, University of Illinois Chicago, Chicago 60612, 801 S. Paulina St, IL, USA.

Tel: 312-413-0239

Fax: 312-996-6044

Email: chungsh@uic.edu

Keywords: BDNF, Dental caries, Dentinogenesis, Regeneration, TrKB, TNFα.

Abstract

Dental caries is one of the most common health issues worldwide arising from the complex interactions of bacteria. In response to harmful stimuli, desirable outcome for the tooth is the formation of tertiary dentin, a protective reparative process that generates new hard tissue. This reparative dentinogenesis is associated with significant inflammation, which triggers the recruitment and differentiation of dental pulp stem cells (DPSCs). Previously, we have shown that brain-derived neurotrophic factor (BDNF) and its receptor TrkB, key mediators of neural functions, are activated during the DPSC-mediated dentin regeneration process. In this study, we further define the role of inflammation in this process and apply stem cell engineering to enhance dentin regeneration in injured teeth. Our data show that TrkB expression and activation in DPSCs rapidly increase during odontogenic differentiation, further amplified by inflammatory inducers and mediators such as TNFα, LTA, and LPS. An in vivo dentin formation assessment was conducted using a mouse pulp-capping/caries model, where CRISPR-engineered DPSCs overexpressing BDNF were transplanted into inflamed pulp tissue. This transplantation significantly enhanced dentin regeneration in injured teeth. To further explore potential downstream pathways, we conducted transcriptomic profiling of TNFα-treated DPSCs, both with and without TrkB antagonist CTX-B. The results revealed significant changes in gene expression related to immune response, cytokine signaling, and extracellular matrix interactions. Taken together, our study advances our understanding of the role of BDNF in dental tissue engineering using DPSCs and identifies potential therapeutic avenues for improving dental tissue repair and regeneration strategies.

Introduction

Dental caries, commonly known as tooth decay, remains one of the most prevalent chronic diseases, affecting a significant portion of the global population (Peres et al., 2019). This condition results from the complex interplay between bacterial biofilms, dietary sugars, and host factors, leading to the demineralization of tooth enamel and dentin (Bowen et al., 2018; Mosaddad et al., 2019). In recent years, there has been growing interest in the role of dental pulp stem cells (DPSCs) in regenerative dentistry due to their ability to differentiate into dentin-forming odontoblast-like cells and their potential in tooth repair and regeneration (Potdar & Jethmalani, 2015). It is widely recognized that the regeneration of the dental-pulp complex is closely associated with inflammation, especially since dental caries and the subsequent regenerative processes take place within an inflammatory environment (Galler et al., 2021). Inflammation serves as a vital biological response for ensuring host survival in the face of infection and tissue injury, playing a crucial role in maintaining normal tissue homeostasis (Peiseler & Kubes, 2018). It is generally accepted that the regeneration of the injured tooth is closely tied to inflammation (Lin & Rosenberg, 2011). Specifically, it plays a pivotal role in the regeneration of injured dental tissues by stimulating the recruitment, proliferation, and differentiation of pulp progenitor cells and odontoblasts (Nakashima et al., 2013). However, an imbalance between inflammation and repair can lead to irreversible tissue damage. While inflammation is recognized as necessary for proficient tissue regeneration, only a few studies have explored its role in dentin regeneration.

The brain-derived neurotrophic factor (BDNF) and its receptor, tropomyosin receptor kinase B (TrkB), constitute a critical signaling pathway involved in the survival, development,

and function of neurons (F. Zhang et al., 2012). Emerging evidence suggests that the BDNF-TrkB pathway also plays a significant role in the inflammatory response and tissue repair processes (Cappoli et al., 2020; Hang et al., 2021). The overexpression of BDNF in DPSCs has been shown to enhance their regenerative capabilities, which may be particularly beneficial in the context of dental caries where inflammation and tissue damage are prominent. Indeed, our previous study demonstrated the critical role of BDNF/TrkB in the DPSC odontoblastic differentiation under inflammation. (Kim, Irfan, Hossain, George, et al., 2023) TNFα (Tumor Necrosis Factor-alpha)-stimulated BDNF/TrkB showed an enhanced odontoblast differentiation of DPSCs.

Although the general principles for successful BDNF-induced regeneration have been proposed, achieving clinical success remains challenging. One significant obstacle is the clinical application of BDNF itself, as the recombinant protein has an extremely short half-life, which greatly diminishes its effectiveness (Miranda-Lourenço et al., 2020). Therefore, establishing a stable and continuous BDNF production platform is essential, and stem cell engineering could potentially address this critical need in the future. Considering the essential role of BDNF/TrkB signaling activation in the inflammatory dentinogenesis observed in cell culture conditions, there is a strong case for validating BDNF/TrkB data in vivo. In this study, we further explore the role of various inflammatory agents in modulating two BDNF receptors, TrkA and TrkB, as well as the potential therapeutic applications of BDNF overexpression in DPSCs using CRISPR technology for the treatment of dental caries. By uncovering the mechanisms through which the BDNF-TrkB pathway affects DPSC function and inflammation, we aim to offer insights into innovative regenerative strategies that could enhance dental health outcomes.

85

86

Result

Various inflammatory mediators increase TrkB expression and activation in DPSCs

Our previous study demonstrated that TNFα augments the odontoblast differentiation of DPSCs in a TrkB-dependent manner (Irfan & Chung, 2023; Kim, Irfan, Hossain, George, et al., 2023). The literature indicates that pro-inflammatory cytokines, such as TNFα, LTA (lymphotoxin-alpha), and LPS (lipopolysaccharides), play significant roles in the formation of tertiary dentin (Irfan, Kim, Marzban, et al., 2022). To further confirm the role of inflammation in this process, various inflammatory mediators were applied during DPSC odontoblastic differentiation. The outline of the experimental timeline is shown (Figure 1A). Human DPSCs were seeded on Day 0, followed by culture in normal growth media. On Day 3, the cells were transferred to dentinogenic media. TNFα, LTA, and LPS treatments were initiated every other three days. The representative image shows the immunofluorescence staining results for TrkB and phosphorylated TrkB (p-TrkB) under various treatments (Figure 1B). The quantification of fluorescence intensity across these different treatment groups was analyzed by percentages of control (Figure 1C). TrkB expression and activation in DPSCs were significantly upregulated during odontogenic differentiation, especially under inflammatory stimulants such as TNFα, LTA, and LPS by 301 ± 17, 320 ± 15.2, and 250 ± 19, respectively vs control 165 ± 12.4 ($p < 0.01$). The spatial distribution of fluorescence intensity for TrkB and p-TrkB was measured across different treatment groups (Figure 1D). Figures were analyzed using ZEN (blue) software, and graphs were created. This spatial analysis confirms the enhanced and localized expression of TrkB and p-TrkB in response to inflammatory stimuli.

Next, we examined the expression levels of TrkA and TrkB receptors in response to various inflammatory stimuli in normal and dentinogenic media. The results indicate significant differential expression of these receptors under both conditions. TrkB expression was modulated by the media and stimuli (Figure 2C). Under control conditions, no significant differences were observed between the media types. However, LPS, LTA, TNFα, and C5a significantly increased TrkB expression in dentinogenic media compared to normal media ($p < 0.001$ for LPS, TNFα, and C5a; $p < 0.05$ for LTA). IL-5 caused a slight but significant increase in TrkB expression in dentinogenic o media ($p < 0.05$). Conversely, baseline TrkA expression showed no significant difference between normal and dentinogenic media (Figure 2A), and C5a and IL-5 did not induce significant changes in TrkA expression in either medium.

Figures 2B and 2D show the effect of TNFα stimulation on the expression of TrkA and TrkB and their phosphorylation vs control. 2D and 2.5 models show fluorescence spikes to evident the phenomenon. It is obvious that TNFα stimulation caused significant phosphorylation of TrkB ($p < 0.01$) compared to TrkA ($p < 0.05$). Graphs (Fig. 2B1 and D1) show significant changes among TNFα treated cells vs control. So, we chose TrkB as a target receptor for our further study.

The dose-dependent response of TrkB to TNFα (Figure 2E) revealed minimal baseline expression at 0 ng/mL TNFα, with significant increases at 0.1 ng/mL, 1 ng/mL, and a pronounced peak at 10 ng/mL in dentinogenic media ($p < 0.001$). At 20 ng/mL TNFα, TrkB expression remained significantly higher in dentinogenic media compared to normal media ($p < 0.001$). The time-dependent response to a fixed TNFα concentration (10 ng/mL) showed that TrkB expression in dentinogenic media was significantly higher on day 1, further increased by

day 3, and peaked on day 7 ($p < 0.001$) (Figure 2F). Although TrkB levels slightly decreased on days 10 and 14, they remained significantly elevated compared to normal media. These findings emphasize the importance of the local microenvironment in influencing receptor expression and inflammatory responses.

TrkB expression is increased in human carious teeth and in DPSCs

Regenerative odontogenic differentiation in the context of caries occurs within an inflammatory environment, making it essential to understand the impact of inflammation on DPSCs to comprehend dentin regeneration fully (Kim, Irfan, Hossain, Shin, et al., 2023). Immunofluorescence double staining was employed to analyze the expression of STRO-1, which is a stem cell marker, and TrkB in human carious and normal teeth, as well as in DPSCs (Fig. 3A-K). The in vivo analysis revealed that STRO-1 was primarily localized around blood vessels, while TrkB was more abundantly expressed in the inflamed pulp tissue of carious teeth compared to normal teeth. Quantitative analysis revealed significantly higher TrkB expression in carious teeth ($p < 0.001$). In vitro, both STRO-1 and TrkB were expressed in control DPSCs, but TNFα treatment markedly increased TrkB expression (Fig. 3L-T). The data showed that TrkB expression was significantly elevated in TNFα-treated DPSCs ($p < 0.01$). These findings suggest that TrkB is upregulated in response to inflammation in both carious teeth and DPSCs.

Transplantation of GFP-tagged CRISPR-engineered BDNF-overexpressing DPSCs enhances dentin regeneration in a pulp-capping mouse model

Our previous data demonstrated that inflammation and BDNF-induced DPSC odontogenic differentiation increased the expression of odontogenic differentiation markers. (Kim, Irfan, Hossain, George, et al., 2023). To investigate whether BDNF-TrkB signaling

controls dentin regeneration following inflammation in vivo, we utilized CRISPR-engineered BDNF-overexpressing DPSCs in a pulp-capping mouse model (Figure 4A). We initially utilized the Clustered Regularly Interspaced Short Palindromic Repeats (CRISPR) technique to activate BDNF expression in DPSCs. Transfection of DPSCs with the BDNF CRISPR activation plasmid was confirmed through Western blot analysis, which revealed increased BDNF expression compared to the control group (Figure 4B). Quantification of the integrated intensity relative to beta-actin further indicated a significant increase in BDNF expression in CRISPR-activated DPSCs (Figure 4C). Histological analysis of H&E-stained sections was performed to evaluate tissue morphology and surgery site from the transplantation of CRISPR-engineered BDNF-overexpressing DPSCs in a pulp-capping mouse model (figure 4D).

Following confirmation of successful CRISPR activation, we conducted the transplantation of CRISPR-engineered BDNF-overexpressing DPSCs on dentin regeneration in a pulp-capping mouse model. Micro-computed tomography (micro-CT) imaging was utilized to assess dentin volume in both sham control and experimental groups. The sham control group [Figure 5A(a-h)] exhibited a clear demarcation of the injured dentin area, highlighted by the white arrow indicating the drilling operation and the dotted line specifying the damaged region. In contrast, the experimental group treated with CRISPR-engineered BDNF-overexpressing DPSCs [Figure 5A(i-p)] showed a notable increase in dentin formation at the injury site. A quantitative analysis of dentin density (Figure 5D) revealed a significant increase in the dentin volume in the group treated with CRISPR-engineered BDNF-overexpressing DPSCs compared to the sham control group. Specifically, the dentin volume in the treated group (Figure 5C) was 1241 ± 51 mg HA/ccm, significantly higher than the control group (Figure 5B), which measured at 1169 ± 9 mg HA/ccm ($p < 0.05$).

To evaluate morphological changes after transplantation, H&E staining was employed to assess cellular and structural changes in the dentin and pulp tissue following the transplantation of CRISPR-engineered BDNF-overexpressing DPSCs in the pulp-capping mouse model. Figure 5 displays representative images of the sham control group and surgery group. The overall morphology of the tooth structure (Figure 4D) and higher magnifications of the injured area highlighted by the box are provided (Figure 5). In contrast to the control group, the BDNF-DPSC transplantation group demonstrated significant dentin regeneration and repair. The newly formed dentin at the injury site appears more organized and closely resembles the native dentin structure.

GFP staining allowed us to identify and localize the transfected areas within the injury site (Figure 5-6). Specifically, GFP expression was observed in areas correlating with the injury compared to the control (Figure 6A). This confirmed the successful transfection and localization of the CRISPR-engineered DPSCs in the mandible of the mouse tooth. line graphs show colocalizations of GFP-tagged DPSCs expressing BDNF and TrkB (Figure 6B). These results indicate that DPSCs overexpressing BDNF, engineered using CRISPR and transplanted into a pulp-capping mouse model, significantly improve dentin regeneration.

RNA sequencing of TNFα-induced DPSCs odontogenic differentiation mediated by TrkB

In our investigation of the combination of TNFα and CTX-B treatment compared to the control, we further aimed to identify the transcriptomic differences associated with the involvement of the BDNF-TrkB pathway related to inflammation. The gene heatmap and transcripts heatmap revealed distinct high and low gene expression patterns between the control and TNFα + CTX-B groups (Figure 7A-B). The volcano plot of differentially expressed genes

(DEGs) illustrated the significant downregulation and upregulation in gene expression between the control and TNFα + CTX-B groups (Figure 7C-D).

We identified significantly enriched Gene Ontology (GO) terms in the categories of biological process, cellular component, and molecular function between these groups (Figure 7E). Notably, there was a distinct difference in membrane-related cellular functions and molecular functions related to protein binding. The GO enrichment pathway analysis revealed that the highest p-values were associated with the extracellular space and region (Figure 8A). Furthermore, Reactome pathway analysis indicated high p-values for pathways related to TNF signaling (Figure 8B).

Sashimi plots comparing control and TNFα + CTX-B treated dental pulp stem cells (DPSCs) highlighted differentially spliced exons in genomic regions of interest (Figure 6D, E, F). The transcriptional response of TNFα + CTX-B treated odontoblast-like differentiated DPSCs showed significant downregulation in TCFs and ATF4 and upregulation in signal transducers and activators of STAT1 and STAT3 (Figure 8C). These findings suggest that TNFα and CTX-B treatment induces significant transcriptomic alterations, particularly affecting pathways involved in cellular signaling and extracellular matrix interactions.

Materials and methods

Chemicals and reagents

Human DPSCs were purchased from Lonza, Pharma & Biotech (Cat. # PT-5025). MEM-alpha, DMEM, PBS, fetal bovine serum, L-glutamine, and Antibiotic–Antimycotic were procured from Gibco™ Fisher Scientific (Waltham, MA, USA). Poly-D-Lysine coated (BioCoat™, 12 mm) round German glass coverslips were purchased from Corning™ Fisher Scientific (Cat. # 354087; Waltham, MA, USA). RIPA buffer was from Cell Signaling Technology (Danvers, MA, USA). Various antibodies were procured: anti-TrkA, anti-phospho-TrkA, anti-TrkB, anti-phospho-TrkB, anti-BDNF, and β-tubulin from BioLegend (San Diego, CA, USA), and anti-β-actin from Fisher Scientific (Waltham, MA, USA), anti-GFP and anti-STRO-1 from Santa Cruz (Dallas, Texas, USA). Fluorescent secondary antibodies were from Life Technologies (Grand Island, NY, USA). TNFα was from Invitrogen, Fisher Scientific (Waltham, MA, USA), and a few other chemicals were from Fisher Chemical (Nazareth, PA, USA). BDNF CRISPR activation plasmid (h) (Cat# sc-400029-ACT) and Reagent System were purchased from Santa Cruz Biotechnology (Dallas, TX, USA).

Cell culture

All experiments were conducted with different sets of human dental pulp stem cells (DPSCs) 3-4 times, using cells at the 2nd and 3rd passages and cell proliferation was measured by counting the total number of cells. Commercially available human DPSCs isolated from third molars of adult donors (ages 29-30 years old) collected during the extraction of wisdom teeth, which were guaranteed through 10 population doublings, to express CD105, CD166, CD29, CD90, and CD73, and do not express CD34, CD45, and CD133 106−108; cultured in regular

growth media (αMEM containing 10% FBS, 1% L-glutamine, and 1% antimycotic/antibiotic) at 37˚C and 5% CO_2 for 3-4 days. After this initial period, the media was swapped to odontogenic media (DMEM containing 10% FBS, 1% L-glutamine and antimycotic/antibiotic, 50 μg/mL ascorbic acid, 10 mM β-glycerophosphate, and 10 nM dexamethasone) at day 4 until day 17. TrkB antagonist (CTX-B, 200nM/ml) was treated every three days until day 17. Cells were treated with LPS, TNFα, LTA, C5a, and IL-5 at days 4 and 7. The CaMKII inhibitor (5 μM/mL), or CaMKII protein (1 μM/mL) were treated with dentinogenic media at days 4, 7, 10, and 14.

Quantitative real-time PCR analysis of odontogenic differentiation marker gene expression in dental pulp stem cells

DPSCs were cultured in a 6-well plate at 5×10^4 cells per well. The total mRNA was extracted using a RNeasy Mini Kit (74104, Qiagen), and the containing quantity of cDNA was measured using the NanoDrop 2000 (ND2000, Fisher Scientific). The Fast SYBR™ Green Master Mix (4385616, ThermoFisher) was used to identify the cDNA sample according to the manufacture′s protocol. Primer sequences (Integrated DNA Technologies) were used predesigned hGAPDH. (Forward: 5′-GGC ATC CAC TGT GGT CAT GAG-3′, Reverse: 5′-TGC ACC ACC AAC TGC TTA GC-3′), hDSPP (Forward: 5′-CTG TTG GGA AGA GCC AAG ATA AG-3′, Reverse: 5′-CCA AGA TCA TTC CAT GTT GTC CT-3′), and hDMP-1 (Forward: 5′-CAC TCA AGA TTC AGG TGG CAG-3′, Reverse: 5′-TCT GAG ATG CGA GAC TTC CTA AA-3′).

Immunocytochemistry

256 The seeded DPSCs were incubated in a 12-well plate with coverslips at 37°C in a CO_2
257 incubator until reaching 70-80% cell confluency. The coverslips were then fixed with 4%
258 paraformaldehyde for 2 hours at 4°C. Blocking and permeabilization were performed using 5%
259 normal goat serum and 0.01% Triton X in 0.01 M phosphate buffer solution (PBS) for 1 hour at
260 room temperature. For primary antibody treatment, the specimens were treated overnight at 4°C
261 with the following antibodies diluted in 5% serum: anti-TrkB (1:1000), anti-pTrkB (1:1000),
262 and/or anti-STRO1 (1:1000). After the overnight incubation with primary antibodies, the
263 secondary antibodies were applied for 2 hours with Alexa Fluor-594 anti-mouse IgG, Alexa
264 Fluor-488 anti-rabbit IgG (1 μg/mL), and/or DAPI (1 μg/mL). The coverslips were mounted on
265 glass slides, and images were taken using a Leica microscope. MATLAB (R2022a) software was
266 used to measure fluorescence intensity and perform quantification.

267 ***BDNF CRISPR Activation Plasmid Transfection in hDPSCs***

268 DPSCs were incubated in a 6-well plate with 3 ml of antibiotic-free standard growth
269 medium at 37°C in a 5% CO2 incubator until reaching 40-60% confluency in preparation for
270 CRISPR activation plasmid transient transfection. For the preparation of transfection solutions, 2
271 μg of plasmid DNA was diluted in Plasmid Transfection Medium (sc-108062) to a final volume
272 of 150 μl (Solution A) and mixed and incubated for 5 minutes at room temperature. In parallel,
273 10 μl of UltraCruz® Transfection Reagent (sc-395739) was diluted in Plasmid Transfection
274 Medium (sc-108062) to a final volume of 150 μl (Solution B) and incubated for 5 minutes at
275 room temperature. Solutions A and B were then combined by vortexing immediately and
276 incubated for 20 minutes at room temperature. For the transfection procedure, the cell culture
277 medium was replaced with a fresh antibiotic-free growth medium, and 300 μl of the Plasmid
278 DNA/UltraCruz® Transfection Reagent Complex was added to each well. The cells were

279 incubated for 48 hours under standard culture conditions. Protein analysis was conducted to
280 confirm overexpression.

281 ***Western blot***

282 To verify BDNF activation using CRISPR plasmid, cell lysates were prepared using RIPA
283 buffer (50 mM Tris pH 7.6, 150 mM NaCl, 1% Triton X100, 1mM EDTA, 0.5% sodium
284 deoxycholate, 0.1% SDS) containing protease inhibitor (Roche, Indianapolis, IN) and protein
285 was measured using BCA method (Pierce™ BCA Protein Assay Kit, Thermo Fisher Scientific,
286 Lenexa, KS). Equal amounts of protein (35 μg) were loaded and separated by SDS-
287 polyacrylamide gel electrophoresis and transferred onto nitrocellulose (Bio-Rad, CA). Blots were
288 probed using polyclonal antibodies specific for BDNF or β-actin for overnight at 4°C and then
289 washed and probed with secondary antibodies for 2 hours at RT. Odyssey CLx visualized the
290 protein bands.

291 ***In cell Western assay***

292 Human DPSCs were seeded in growth media at 15×10^3 cells/cm^2 in 96-well optical
293 plates. At sub-confluency, cells were incubated in an antibiotic-free medium and treated as
294 mentioned above. Then, cells were immediately fixed with 100% cold methanol (15 min) and
295 saturated with 5% BSA (1.5 h). Cells were incubated overnight at 4 °C, anti-TrkA, anti-TrkB,
296 anti-phospho-TrkA, anti-phospho-TrkB, or anti-β-tubulin. Cells were then washed (0.05%
297 Tween-20/PBS) and incubated with respective IRDye-680RD or IRDye-800RD secondary
298 antibody (1 h) at RT. After 5 washes, plates were dried and scanned at 700 and/or 800 nm
299 (Odyssey CLx).

300 ***Animals***

301 The Institutional Animal Care and Use Committee (IACUC) at the University of Illinois
302 Chicago reviewed and approved all surgical and experimental procedures. C57BL/6 male mice,
303 6-8 weeks old (n = 12), were used for the experiments and purchased from Jackson Laboratory
304 (#000461). The animals were housed in three per cage in a temperature-controlled room (23 ± 1
305 °C, 12 h/12 h light/dark cycle) and maintained at the UIC animal facility. For the mouse molars,
306 the mandibles of the C57BL/6 mice were collected for further experimentation (Protocol no.: 21-
307 197).

308 ***Transplantation of CRISPR-engineered BDNF-overexpressing DPSC in the pulp-***
309 ***capping mouse model (In-Vivo)***

310 C57BL/6 male mice aged 6 to 8 weeks were employed for this mouse model. Dentin of
311 the lower left first molar was penetrated using a 0.3 mm rounded carbide burr drill operating at
312 automatic speed. Subsequently, an 11 G needle was utilized to remove any remaining dentin
313 upon exposure. The exposed dentin was then treated with BDNF CRISPR Activation Plasmid-
314 transfected DPSCs embedded in collagen (from rat tail), followed by sealing with mineral
315 trioxide aggregate (MTA) to shield the pulp from further inflammation. Animals were euthanized
316 beginning 4 weeks post-injury, and their mandibles were excised. The molars were subsequently
317 harvested for histological, molecular, and immunohistochemical analyses to evaluate the efficacy
318 of the treatment in promoting dental pulp regeneration.

319 ***Micro-computed tomography (µCT)***

320 Mandibles from C57BL/6 male mice were collected from both the sham control group
321 and the group receiving transplantation of CRISPR-engineered BDNF-overexpressing dental
322 pulp stem cells (DPSCs) in the pulp-capping mouse model. Micro-CT (µCT) analyses were

323 conducted using the commercial service at RUSH Hospital to assess the volume of regenerated
324 dentin quantitatively. All animal phenotype analyses were blinded to mitigate potential examiner
325 bias and ensure impartial evaluation.

326 ***Hematoxylin and eosin staining (H&E staining)***

327 The mandibles of C57BL/6 mice were harvested and fixed in a 4% formaldehyde
328 solution immediately after extraction. Subsequently, they were placed in decalcification solution
329 within 15 mL Falcon tubes for two days, with daily changes in concentration (starting from 10%
330 sucrose in PBS, progressing to 20% and then 30%). The mandibles were sectioned following
331 decalcification, and histological staining protocols were optimized specifically for dental tissues.
332 Sections underwent a sequence of staining procedures, including bleaching, eosin staining, and
333 dehydration through graded ethanol solutions (ranging from 70% to 100% ethanol). Finally, the
334 sections were cleared in xylene to prepare them for microscopic analysis and further
335 histopathological evaluation.

336 ***Collection of human virgin teeth and caries teeth***

337 Human wisdom tooth extractions were conducted by licensed dentists specializing in oral
338 surgery . This study involving human specimens received ethical approval from the Endodontics
339 clinic at the College of Dentistry, University of Illinois Chicago (Protocol no.: 2012-0588). Prior
340 to participation, all patients provided informed written consent detailing the nature and
341 objectives of the experimental procedures. Ethical considerations and patient confidentiality
342 were strictly followed throughout the study, ensuring compliance with established guidelines and
343 protocols for human research.

344 ***Immunohistochemistry***

The extracted mandibles were embedded in an OCT cryostat sectioning medium and stored at -20°C for 2 hours before being cut into 20 µm thick sections. The mounted tissues were fixed with 4% paraformaldehyde for 1 hour at room temperature. Subsequently, blocking and permeabilization were performed using 10% normal goat serum (NGS) and 0.1% Triton X in 0.01 M phosphate buffer solution (PBS) for 1 hour at room temperature. For primary antibody incubation, the specimens were treated overnight at 4°C with mouse anti-CaMKII (1:200), rabbit anti-p-CaMKII (1:200), mouse anti-GFAP (1:200), and/or mouse anti-STRO1 (1:200), diluted in 10% NGS. Following overnight incubation with primary antibodies, the specimens were incubated for 2 hours at room temperature with secondary antibodies: Alexa Fluor-594 anti-mouse IgG, Alexa Fluor-488 anti-rabbit IgG (1 µg/mL), and/or DAPI (3 µg/mL). After secondary antibody treatment, the specimens were mounted on glass slides, and images were acquired using a Leica microscope. Fluorescence intensity was quantified using Image J software. Representative images were exported in TIFF format. Image J software and GraphPad Prism version 10 were employed for fluorescence intensity analysis.

RNA Sequencing (Poly-A RNA Seq)

RNA Sequencing was employed to comprehensively analyze the transcriptome, focusing specifically on mRNA, utilizing services provided by LC Biosciences (Houston, Texas). This method capitalizes on the polyadenylated (poly-A) tails present at the 3' ends of eukaryotic mRNA molecules. Dental pulp stem cells (DPSCs) underwent a 10-day differentiation protocol with or without specific treatments. Post-differentiation, total RNA was extracted from the odontogenic differentiated DPSCs for sample preparation. LC Biosciences conducted rigorous assessments to evaluate the extracted RNA's quantity and quality, followed by poly-A selection to enrich for mRNA transcripts. Subsequent cDNA synthesis facilitated library preparation,

368 paving the way for high-throughput sequencing to explore the transcriptomic landscape in depth.
369 This approach enabled the identification and characterization of gene expression patterns
370 associated with the differentiation of DPSCs under various experimental conditions.

371 ***Statistical analysis***

372 The statistical analyses were performed on at least 3 independent experiments with
373 duplicates or triplicates, and statistical significance was determined using one-way analysis of
374 variance (ANOVA) followed by post-hoc Dunnett's test (SAS 9.4) to compare the different
375 treatments and their respective controls (p-value of 0.05 or less was considered statistically
376 significant). In addition, the data were analyzed using Tukey's test to determine statistical
377 significance between the groups. For quantification of immunofluorescence staining intensity,
378 ImageJ 1.49v software was used. Fixed areas of 1 mm × 1 mm or 2 mm × 2 mm were selected to
379 analyze differentiated cells' number or fluorescence intensity.

380

381

Discussion

Odontoblastic differentiation of DPSCs in response to caries injury takes place within an inflammatory environment (Chmilewsky et al., 2016). However, there is still limited information on the role of inflammation in reparative dentinogenesis and the biology of DPSCs. Our findings demonstrate the activation of TrkB during the caries process. Consistent with this, our in vitro data confirmed that various inflammatory mediators increase TrkB expression and activation in DPSCs. These findings suggest that BDNF/TrkB directly affects the pulpal response to caries. In vivo, TrkB is more highly expressed in inflamed pulp compared to normal tissue. The transplantation of CRISPR-engineered BDNF-overexpressing DPSCs in a pulp-capping mouse model significantly enhances dentin regeneration and repair, as demonstrated by increased dentin volume and improved tissue morphology. Furthermore, RNA sequencing reveals significant transcriptomic changes in TNFα-treated DPSCs, affecting cellular signaling and extracellular matrix pathways. These results underscore the critical role of TrkB in inflammatory responses and dentin repair, suggesting potential for targeted TrkB modulation in dental tissue regeneration.

TNFα and LTA are known to mediate inflammatory responses and contribute to the recruitment and activation of immune cells at the injury site (Farges et al., 2015; Kawai & Akira, 2010). This inflammatory response is crucial for eliminating pathogens and debris, setting the stage for tissue repair. In the context of dentin formation, these cytokines promote the differentiation and activity of odontoblast-like cells, which are responsible for producing the reparative dentin matrix. (Durand et al., 2006; Keller et al., 2010) Lipopolysaccharides (LPS), components of the outer membrane of Gram-negative bacteria, also stimulate an inflammatory response when they infiltrate the dental pulp. (Brodzikowska et al., 2022) The presence of LPS

triggers the release of various pro-inflammatory cytokines, further enhancing the recruitment of immune cells and promoting the processes necessary for tertiary dentin formation. (Widbiller et al., 2018) These pro-inflammatory cytokines coordinate a complex cascade of events that lead to the regeneration of dentin, highlighting their importance in dental tissue repair mechanisms.

Our study confirms the impact of pro-inflammatory stimuli on the expression and activation of TrkB in DPSCs. Immunofluorescence analysis (Figure 1) demonstrated that exposure to LPS, LTA, and TNFα significantly upregulated both TrkB and its phosphorylated form, p-TrkB, compared to the control. This suggests that these inflammatory agents can activate TrkB signaling pathways in DPSCs, potentially influencing their behavior and differentiation. TNFα showed the most pronounced effect, indicating its potent role in activating TrkB signaling. These findings are consistent with previous studies indicating that TNFα can enhance TrkB expression and activation in various cell types, promoting cellular responses to inflammation (Irfan et al., 2024; Kim, Irfan, Hossain, George, et al., 2023; Paula-Silva et al., 2009). These results suggest that pro-inflammatory stimuli such as LPS, LTA, and TNFα can significantly enhance TrkB and p-TrkB expression in DPSCs.

Furthermore, our data demonstrate that significant upregulation of TrkA and TrkB expressions in dentinogenic media in response to inflammatory components. TrkB expression was notably increased by LPS, LTA, TNFα, and C5a, suggesting widespread receptor activation. This upregulation may play a critical role in mediating the cellular responses to inflammation, potentially influencing the behavior of DPSCs in the context of dental pulp inflammation and regeneration. Particularly, TNFα induced the highest TrkB upregulation in both media types, emphasizing the role of TrkB in mediating responses to neurotrophic factors and involvement in

inflammatory pathways (Irfan, Kim, Druzinsky, et al., 2022). The differential expression in dentinogenic media indicates enhanced receptor sensitivity and signaling in an inflammatory environment (J. Zhang et al., 2016). A dose-dependent increase in TrkB expression was observed with escalating TNFα concentrations, with significant upregulation at 10 ng/mL, beyond which further increases in TNFα did not enhance expression. This suggests that higher doses are unnecessary to avoid inflammation related to degeneration or infection (Kim, Irfan, Hossain, George, et al., 2023). The time-dependent response to a fixed TNFα concentration showed a peak at day 7, indicating that a minimum of 7 days of differentiation is necessary for culturing DPSCs in inflammatory responses related to TrkB expression. In vivo, TrkB expression was significantly higher in the inflamed pulp tissue of carious teeth, indicating that TrkB may play a critical role in the response to dental caries and pulp inflammation. This suggests that BDNF-TrkB signaling could be crucial in the neurogenic and angiogenic processes involved in pulp tissue repair (Bar et al., 2021; De Moraes et al., 2018).

The transplantation of CRISPR-engineered BDNF-overexpressing DPSCs has demonstrated promising results in enhancing dentin regeneration in a pulp-capping mouse model. Both micro-CT images and H&E staining analyses indicate that the overexpression of brain-derived neurotrophic factor (BDNF) via CRISPR engineering significantly promotes dentin repair at the injury site. BDNF is known for its role in molecular and physiological involvement (Lu et al., 2014). Its application in dental tissue engineering suggests that it may also play a crucial role in odontogenesis and dentinogenesis (Kim, Irfan, Hossain, George, et al., 2023). The significant increase in dentin volume in the micro-CT experiment observed in this study supports the hypothesis that BDNF can enhance the regenerative capabilities of DPSCs, leading to improved outcomes in dentin repair. Enhanced dentinogenesis was evidenced by the well-

organized and structurally similar new dentin formation in the transplantation group compared to the native dentin structure. The histological analysis with H&E staining further verified these findings, showing a marked improvement in dentin formation and reduced inflammation in the BDNF-DPSC transplantation group compared to the control group. This suggests that BDNF enhances dentin regeneration, creating a conducive environment for tissue repair. Several potential mechanisms could explain that BDNF may enhance the proliferation and differentiation of DPSCs into odontoblast-like cells, promoting reparative dentin formation (Tsutsui, 2020). Moreover, the neurotrophic properties of BDNF could support the survival and function of sensory nerve fibers within the pulp, which may play a role in regulating the repair process (Bathina & Das, 2015).

In vitro experiments with DPSCs further supported these findings, demonstrating that TrkB expression is significantly upregulated in response to TNFα treatment. This suggests that inflammation enhances the neurogenic potential of DPSCs through TrkB signaling. The co-expression of TrkB in both carious teeth and DPSCs highlights the potential of targeting the BDNF-TrkB pathway in dental regenerative therapies. Modulating the inflammatory environment to enhance TrkB signaling could improve the regenerative properties of DPSCs, offering promising strategies for managing dental caries and pulpitis. The combined treatment of TNFα and CTX-B elucidates the significant transcriptional reprogramming compared with the control. The volcano plots highlight a substantial number of differentially expressed genes (DEGs), indicating both upregulation and downregulation of gene expression compared to control. The GO enrichment analysis reveals that these DEGs are predominantly associated with biological processes such as extracellular matrix organization, inflammatory response, and cytokine-mediated signaling pathways. This is further supported by the GO term statistics, where

notable terms like extracellular space and cartilage homeostasis are enriched, suggesting alterations in the cellular microenvironment and immune response.

Additionally, the pathway enrichment analysis identifies critical pathways such as TNF signaling, NF-κB signaling, and cytokine-cytokine receptor interaction, underscoring the crucial role of inflammatory signaling in the observed transcriptional changes. Finally, the gene expression analysis under TNFα + CTX-B treatment provides specific examples of genes with altered expression patterns, confirming the extensive impact of the treatment at the molecular level. These findings suggest that TNFα treatment mediated by BDNF/TrkB pathway induces a complex network of transcriptional changes that modulate the extracellular matrix and inflammatory signaling pathways.

Conclusion

The findings of this study have significant clinical implications for dental regenerative therapies. The use of CRISPR-engineered BDNF-overexpressing DPSCs could offer a novel and effective approach for enhancing dentin repair and regeneration in cases of dental pulp injury. This approach could potentially reduce the need for more invasive treatments, such as root canal therapy, and improve outcomes for patients with dental trauma or disease. Further studies are necessary to investigate the long-term effects of BDNF overexpression on dentin regeneration and to explore the underlying mechanisms driving this enhanced repair process. Additionally, assessing the potential for clinical translation of this approach will be crucial in determining its viability as a therapeutic option for dental pulp injuries and related conditions.

Data Availability Statement: The datasets generated during and/or analyzed during the current study are available from the corresponding author upon reasonable request.

Author Contributions: J.H.K., M.I., and S.C. contributed to the conception, design, data acquisition, analysis, and interpretation and drafted and critically revised the manuscript. J.H.K and M.I. conducted most of the experiments and contributed to data acquisition and analysis of the experiment, while S.K and A.P. contributed to partial experiments, contributed data analysis, and critically wrote and edited the manuscript. S.C. designed the original concept, contributed to data acquisition and interpretation, and financially supported the project.

Funding: This study was supported by the NIH/NIDCR Grant: R01 DE029816– SC.

Conflicts of Interest: The authors declare no conflict of interest.

Reference:

Bar, J. K., Lis-Nawara, A., & Grelewski, P. G. (2021). Dental Pulp Stem Cell-Derived Secretome and Its Regenerative Potential. *International Journal of Molecular Sciences*, *22*(21), 12018. https://doi.org/10.3390/ijms222112018

Bathina, S., & Das, U. N. (2015). Brain-derived neurotrophic factor and its clinical implications. *Archives of Medical Science: AMS*, *11*(6), 1164–1178. https://doi.org/10.5114/aoms.2015.56342

Bowen, W. H., Burne, R. A., Wu, H., & Koo, H. (2018). Oral Biofilms: Pathogens, Matrix, and Polymicrobial Interactions in Microenvironments. *Trends in Microbiology*, *26*(3), 229–242. https://doi.org/10.1016/j.tim.2017.09.008

513 Brodzikowska, A., Ciechanowska, M., Kopka, M., Stachura, A., & Włodarski, P. K. (2022). Role
514 of Lipopolysaccharide, Derived from Various Bacterial Species, in Pulpitis—A
515 Systematic Review. *Biomolecules*, *12*(1), 138. https://doi.org/10.3390/biom12010138
516 Cappoli, N., Tabolacci, E., Aceto, P., & Dello Russo, C. (2020). The emerging role of the BDNF-
517 TrkB signaling pathway in the modulation of pain perception. *Journal of*
518 *Neuroimmunology*, *349*, 577406. https://doi.org/10.1016/j.jneuroim.2020.577406
519 Chmilewsky, F., About, I., & Chung, S.-H. (2016). Pulp Fibroblasts Control Nerve Regeneration
520 through Complement Activation. *Journal of Dental Research*, *95*(8), 913–922.
521 https://doi.org/10.1177/0022034516643065
522 De Moraes, J. K., Wagner, V. P., Fonseca, F. P., Vargas, P. A., De Farias, C. B., Roesler, R., &
523 Martins, M. D. (2018). Uncovering the role of brain-derived neurotrophic factor/tyrosine
524 kinase receptor B signaling in head and neck malignancies. *Journal of Oral Pathology &*
525 *Medicine*, *47*(3), 221–227. https://doi.org/10.1111/jop.12611
526 Durand, S. H., Flacher, V., Roméas, A., Carrouel, F., Colomb, E., Vincent, C., Magloire, H.,
527 Couble, M.-L., Bleicher, F., Staquet, M.-J., Lebecque, S., & Farges, J.-C. (2006).
528 Lipoteichoic Acid Increases TLR and Functional Chemokine Expression while Reducing
529 Dentin Formation in In Vitro Differentiated Human Odontoblasts. *The Journal of*
530 *Immunology*, *176*(5), 2880–2887. https://doi.org/10.4049/jimmunol.176.5.2880
531 Farges, J.-C., Alliot-Licht, B., Renard, E., Ducret, M., Gaudin, A., Smith, A. J., & Cooper, P. R.
532 (2015). Dental Pulp Defence and Repair Mechanisms in Dental Caries. *Mediators of*
533 *Inflammation*, *2015*, 1–16. https://doi.org/10.1155/2015/230251
534 Galler, K. M., Weber, M., Korkmaz, Y., Widbiller, M., & Feuerer, M. (2021). Inflammatory
535 Response Mechanisms of the Dentine-Pulp Complex and the Periapical Tissues.

International Journal of Molecular Sciences, *22*(3), 1480. https://doi.org/10.3390/ijms22031480

Hang, P.-Z., Zhu, H., Li, P.-F., Liu, J., Ge, F.-Q., Zhao, J., & Du, Z.-M. (2021). The Emerging Role of BDNF/TrkB Signaling in Cardiovascular Diseases. *Life*, *11*(1), 70. https://doi.org/10.3390/life11010070

Irfan, M., & Chung, S. (2023). C5L2 modulates BDNF production in human dental pulp stem cells via p38α pathway. *Scientific Reports*, *13*(1), 74. https://doi.org/10.1038/s41598-022-27320-6

Irfan, M., Kim, J. H., Druzinsky, R. E., Ravindran, S., & Chung, S. (2022). Complement C5aR/LPS-induced BDNF and NGF modulation in human dental pulp stem cells. *Scientific Reports*, *12*(1), 2042. https://doi.org/10.1038/s41598-022-06110-0

Irfan, M., Kim, J.-H., Marzban, H., Reed, D. A., George, A., Cooper, L. F., & Chung, S. (2022). The role of complement C5a receptor in DPSC odontoblastic differentiation and in vivo reparative dentin formation. *International Journal of Oral Science*, *14*(1), 7. https://doi.org/10.1038/s41368-022-00158-4

Irfan, M., Marzban, H., & Chung, S. (2024). C5L2 CRISPR KO enhances dental pulp stem cell-mediated dentinogenesis via TrkB under TNFα-induced inflammation. *Frontiers in Cell and Developmental Biology*, *12*, 1338419. https://doi.org/10.3389/fcell.2024.1338419

Kawai, T., & Akira, S. (2010). The role of pattern-recognition receptors in innate immunity: Update on Toll-like receptors. *Nature Immunology*, *11*(5), 373–384. https://doi.org/10.1038/ni.1863

Keller, J.-F., Carrouel, F., Colomb, E., Durand, S. H., Baudouin, C., Msika, P., Bleicher, F., Vincent, C., Staquet, M.-J., & Farges, J.-C. (2010). Toll-like receptor 2 activation by

559 lipoteichoic acid induces differential production of pro-inflammatory cytokines in human
560 odontoblasts, dental pulp fibroblasts and immature dendritic cells. *Immunobiology*,
561 *215*(1), 53–59. https://doi.org/10.1016/j.imbio.2009.01.009
562 Kim, J.-H., Irfan, M., Hossain, M. A., George, A., & Chung, S. (2023). BDNF/TrkB Is a Crucial
563 Regulator in the Inflammation-Mediated Odontoblastic Differentiation of Dental Pulp
564 Stem Cells. *Cells*, *12*(14), 1851. https://doi.org/10.3390/cells12141851
565 Kim, J.-H., Irfan, M., Hossain, M. A., Shin, S., George, A., & Chung, S. (2023). LPS-induced
566 inflammation potentiates dental pulp stem cell odontogenic differentiation through C5aR
567 and p38. *Connective Tissue Research*, 1–11.
568 https://doi.org/10.1080/03008207.2023.2218944
569 Lin, L. M., & Rosenberg, P. A. (2011). Repair and regeneration in endodontics: Repair and
570 regeneration in endodontics. *International Endodontic Journal*, *44*(10), 889–906.
571 https://doi.org/10.1111/j.1365-2591.2011.01915.x
572 Lu, B., Nagappan, G., & Lu, Y. (2014). BDNF and Synaptic Plasticity, Cognitive Function, and
573 Dysfunction. In G. R. Lewin & B. D. Carter (Eds.), *Neurotrophic Factors* (Vol. 220, pp.
574 223–250). Springer Berlin Heidelberg. https://doi.org/10.1007/978-3-642-45106-5_9
575 Miranda-Lourenço, C., Ribeiro-Rodrigues, L., Fonseca-Gomes, J., Tanqueiro, S. R., Belo, R. F.,
576 Ferreira, C. B., Rei, N., Ferreira-Manso, M., De Almeida-Borlido, C., Costa-Coelho, T.,
577 Freitas, C. F., Zavalko, S., Mouro, F. M., Sebastião, A. M., Xapelli, S., Rodrigues, T. M.,
578 & Diógenes, M. J. (2020). Challenges of BDNF-based therapies: From common to rare
579 diseases. *Pharmacological Research*, *162*, 105281.
580 https://doi.org/10.1016/j.phrs.2020.105281

581 Mosaddad, S. A., Tahmasebi, E., Yazdanian, A., Rezvani, M. B., Seifalian, A., Yazdanian, M., &
582 Tebyanian, H. (2019). Oral microbial biofilms: An update. *European Journal of Clinical*
583 *Microbiology & Infectious Diseases*, *38*(11), 2005–2019. https://doi.org/10.1007/s10096-
584 019-03641-9
585 Nakashima, M., Iohara, K., & Murakami, M. (2013). Dental pulp stem cells and regeneration.
586 *Endodontic Topics*, *28*(1), 38–50. https://doi.org/10.1111/etp.12027
587 Paula-Silva, F. W. G., Ghosh, A., Silva, L. A. B., & Kapila, Y. L. (2009). TNF-α Promotes an
588 Odontoblastic Phenotype in Dental Pulp Cells. *Journal of Dental Research*, *88*(4), 339–
589 344. https://doi.org/10.1177/0022034509334070
590 Peiseler, M., & Kubes, P. (2018). Macrophages play an essential role in trauma-induced sterile
591 inflammation and tissue repair. *European Journal of Trauma and Emergency Surgery*,
592 *44*(3), 335–349. https://doi.org/10.1007/s00068-018-0956-1
593 Peres, M. A., Macpherson, L. M. D., Weyant, R. J., Daly, B., Venturelli, R., Mathur, M. R., Listl,
594 S., Celeste, R. K., Guarnizo-Herreño, C. C., Kearns, C., Benzian, H., Allison, P., & Watt,
595 R. G. (2019). Oral diseases: A global public health challenge. *The Lancet*, *394*(10194),
596 249–260. https://doi.org/10.1016/S0140-6736(19)31146-8
597 Potdar, P. D., & Jethmalani, Y. D. (2015). Human dental pulp stem cells: Applications in future
598 regenerative medicine. *World Journal of Stem Cells*, *7*(5), 839–851.
599 https://doi.org/10.4252/wjsc.v7.i5.839
600 Tsutsui, T. (2020). Dental Pulp Stem Cells: Advances to Applications. *Stem Cells and Cloning:*
601 *Advances and Applications*, *Volume 13*, 33–42. https://doi.org/10.2147/SCCAA.S166759
602 Widbiller, M., Eidt, A., Wölflick, M., Lindner, S. R., Schweikl, H., Hiller, K. -A., Buchalla, W.,
603 & Galler, K. M. (2018). Interactive effects of LPS and dentine matrix proteins on human

dental pulp stem cells. *International Endodontic Journal*, *51*(8), 877–888. https://doi.org/10.1111/iej.12897

Zhang, F., Kang, Z., Li, W., Xiao, Z., & Zhou, X. (2012). Roles of brain-derived neurotrophic factor/tropomyosin-related kinase B (BDNF/TrkB) signalling in Alzheimer's disease. *Journal of Clinical Neuroscience*, *19*(7), 946–949. https://doi.org/10.1016/j.jocn.2011.12.022

Zhang, J., Yao, W., & Hashimoto, K. (2016). Brain-derived Neurotrophic Factor (BDNF)-TrkB Signaling in Inflammation-related Depression and Potential Therapeutic Targets. *Current Neuropharmacology*, *14*(7), 721–731. https://doi.org/10.2174/1570159X14666160119094646

Figure Legends

Figure 1. Effects of various inflammatory mediators on the expression of TrkB and its phosphorylation in human DPSCs.

(A) Schematic representation of DPSC differentiation stimulated by various inflammatory mediators. **(B)** DPSCs were cultured in normal growth media with or without LPS, LTA or TNFα for 24 hours, and cells were fixed, and double immunofluorescent staining was performed (TrkB: red; p-TrkB: green). Cells were counter-stained with DAPI (blue). (a-d) the control cells showed less TrkB and p-TrkB expression than the LPS (e-h), LTA (i-l), or TNFα (m-p) treated groups. **(C)** The bar graph shows a significant increment in TrkB and p-TrkB expression in the groups treated with inflammatory mediators. * $p < 0.05$ and ** $p < 0.01$ vs control. **(D)** The Line graph shows that the co-localization of TrkB and p-TrkB are higher peaks observed in LPS, LTA, and TNFα treated groups than in control. Scale bar: 50 μm.

Figure 2. Time-course analyses of TrkB mRNA expression in DPSCs.

(A and C) Real-time PCR was used to determine the effect of various inflammatory mediators (LPS, LTA, IL5, TNFα, and C5a) on the expression level of TrkA & TrkB mRNA in DPSCs after 1 d treatment in regular growth medium (blue bars) or dentinogenic medium (red bars). While these inflammatory components do not affect much the expression of TrkA or TrkB in normal growth medium, inflammatory mediators such as LPS, LTA, and TNFα stimulation increase TrkB expression in DPSCs undergoing odontoblastic differentiation (orange bars "LPS, LTA & TNFα" vs. orange bar "Control"). Comparatively, TrkA expression changed little during the odontoblastic differentiation of DPSCs (A). **(B and D)** In cell western assay showing effects of TNFα on the expression of TrkA & TrkB and their phosphorylation in 2D and 2.5 D models.

Graphs (B1 and D1) show fluorescence intensity TNFα vs control. **(E)** Effect of TNFα on TrkB expression. DPSCs were cultured in regular or dentinogenic/osteogenic medium and with 0, 0.1, 1, 10, or 20 ng/mL of TNFα. TrkB mRNA expression was determined by real-time PCR analysis after 24 h of culture. TNFα stimulation, independent of the concentration used, quickly potentiates the odontogenesis-regulated expression of TrkB. However, this TrkB expression increase is sustained with increasing concentrations of TNFα treatment, even at 20 ng/mL. **(F)** Real-time PCR was used to evaluate the level of TrkB mRNA in DPSCs after 1, 3, 7, 10, and d 14 of culture in regular medium (blue lines) or dentinogenic medium (orange lines) in TNFα-stimulated DPSCs odontoblastic differentiation. In contrast to relatively stable TrkB levels in undifferentiated DPSCs, TrkB expression quickly increased in dentinogenic medium, with the most significant increase detected between 7 and 10 d (fold increase: 7 d = 12.04 ± 2.1, 10 d = 14.1 ± 1.72). Results are expressed as relative expression to glyceraldehyde 3-phosphate dehydrogenase (GAPDH). Data are presented as mean ± SD of 3 independent experiments. $^{*}P < 0.05$ vs. regular medium, $^{*}P < 0.05$, and ** $p < 0.01$, *** $p < 0.001$ vs. dentinogenic medium and without inflammatory stimulation.

Figure 3. Expression of STRO-1 and TrkB in human carious or normal tooth in vivo and DPSCs in vitro.

(A-J) Immunofluorescence double staining was used to localize STRO-1 and TrkB-expressing cells in the human virgin (control) and carious tooth section. While the expression of STRO-1 was detected in the vicinity of blood vessels, TrkB is expressed more in inflamed pulp tissue compared with virgin tooth. Merged images of STRO-1 and TrkB staining demonstrated a co-expression of TrkB and STRO-1 in the perivascular area. Scale bar: 100 μm. Nuclei were

counterstained with DAPI (blue). **(K)** The bar graph shows a significantly higher expression of TrkB in the carious tooth section (***$p < 0.001$ vs. control). **(L-S)** Expression of STRO-1 and TrkB by DPSCs in vitro. Immunofluorescence double staining was used to analyze TrkB expression in control or untreated and TNFα treated cells. All control DPSCs express both the mesenchymal stem cell marker STRO1 and TrkB, while TNFα treated cells TrkB expression was significantly higher than control. Merged images of STRO1 and TrkB revealed that all STRO-1-positive cells expressed TrkB. Nuclei were counterstained with DAPI (blue). Scale bar = 50 μm. **(T)** The bar graph shows significantly higher expression of TrkB in TNFα treated cells ($p < 0.01$ vs. control).

Figure 4. The transplantation of CRISPR-engineered BDNF-overexpressing DPSCs in the pulp-capping mouse model.

(A) A schematic representation of the transplantation of DPSC into the first molar tooth after drilling. **(B)** The confirmation of BDNF CRISPR activation plasmid enhanced the expression of BDNF. **(C)** Bar graph showing the integrated intensity of CRISPR-engineered BDNF-activated DPSCs against β-actin compared to control. **(D)** H&E staining of sham control and injured tooth in mouse transplanted with CRISPR-engineered BDNF-overexpressing DPSCs.

Figure 5. The transplantation of CRISPR-engineered BDNF-overexpressing DPSCs in the pulp-capping mouse model and micro-CT analysis.

(A) Immunohistochemistry was performed to assess GFP-tagged transplanted cells. The white arrow indicates the pulp lining. **(B)** Micro-computed tomography (micro-CT) image in the Sham control of the pulp-capping mouse model. The white arrow indicates the drilling operation, and the dotted line specifies the injured area of dentin. The white box is a magnified image of the

injured area. **(C)** The transplantation of CRISPR-engineered BDNF-overexpressing DPSCs in the pulp-capping mouse model. **(D)** Analyzed density of dentin compared with Sham control vs. transplantation of CRISPR-engineered BDNF-overexpressing DPSCs in the pulp-capping mouse model. ($p < 0.01$ vs. control).

Figure 6. Detection of BDNF and TrkB in GFP-tagged cells transplanted in the pulp-capping mouse model.

(A) Representative image of Sham control of the pulp-capping mouse model. (a-j) Sham control vs (k-t) representative image of the transplantation of CRISPR-engineered BDNF-overexpressing DPSCs in the pulp-capping mouse model. Scale bars: 25 and 50 μm. **(B)** Line graphs showing the co-localization of BDNF and GFP [B(e1 and j1)] and of TrkB and GFP [B(o1 and t1)].

Figure 7. The total RNA-Seq analysis between normal DPSCs and TNFα + CTX-B treated DPSCs in dentinogenic media.

(A) Heatmap of the differentially expressed genes between normal DPSCs and TNFα + CTX-B DPSCs in dentinogenic media from total RNA-Seq analysis. **(B)** Transcripts heatmap of the differentially expressed genes between normal DPSCs and TNFα + CTX-B DPSCs in dentinogenic media from total RNA-Seq analysis. Color corresponds to log to fold change. Red and yellow stripes in the figure represent high-expression genes, while blue stripes represent low-expression genes. **(C)** Volcano map comparing gene expression between normal DPSCs and TNFα+CTX-B treated DPSCs. **(D)** Volcano map comparing transcripts between normal DPSCs and TNFα+CTX-B treated DPSCs. In both plots, the x-axis represents the log2 fold change in

gene expression, and the y-axis represents the -log10 of the adjusted p-value. Genes or transcripts significantly upregulated are marked in red, and downregulated genes are marked in blue. The dotted horizontal line indicates the threshold for statistical significance, while vertical lines indicate fold change thresholds. **(E)** Significant enriched Gene Ontology (GO) terms among control and TNFα + CTX-B treated DPSCs based on biological process (Blue), cellular function (Green), and molecular function (Orange). Bar chart representing the number of genes associated with significant GO terms. The x-axis lists the GO terms, while the y-axis shows the number of genes enriched for each term.

Figure 8. Signaling pathways affected by TNFα-induced DPSCs mediated by TrkB inhibitor in odontoblasts like differentiation of DPSCs in dentinogenic media.

(A) A dot plot showing the GO terms enriched in the dataset. The size of the dots represents the number of DEGs, while the color indicates the p-value, with darker colors representing more significant enrichment depending on the rich factor, which is the ratio of the number of DEGs annotated in a GO term to the total number of genes annotated in that term. **(B)** the pathways enriched among the DEGs. The x-axis shows the rich factor, and the y-axis lists the pathways. The size of the dot indicates the number of genes involved in each pathway. **(C)** Next-generation RNA sequencing was done using poly-A-RNA sequencing technique. Histogram showing upregulated and activated transcription factors (blue) and repressed or down-regulated transcription factors (orange). Histogram showing the effect of CTX-B on the regulation of various transcription factors. Notably, TCF (7, 12, 19) was abolished with the treatment of CTX-B. **(D-F)** The Sashimi plots show the expression patterns of specific genes in response to TNFα+CTX-B treatment. Data were examined on sashimi plots, which revealed the number of

variants and genomic mutations on chr19, chr12, and chr17 in TNFα+CTX-B treated cells in dentinogenic media against control. Red sashimi plots show variants in the TNFα+CTX-B treated group, and orange shows in the control. The lower black annotations are Read alignments of alternative isoforms and genomic regions of interest providing the gene model, with exons represented as thick blocks and introns as thin lines.

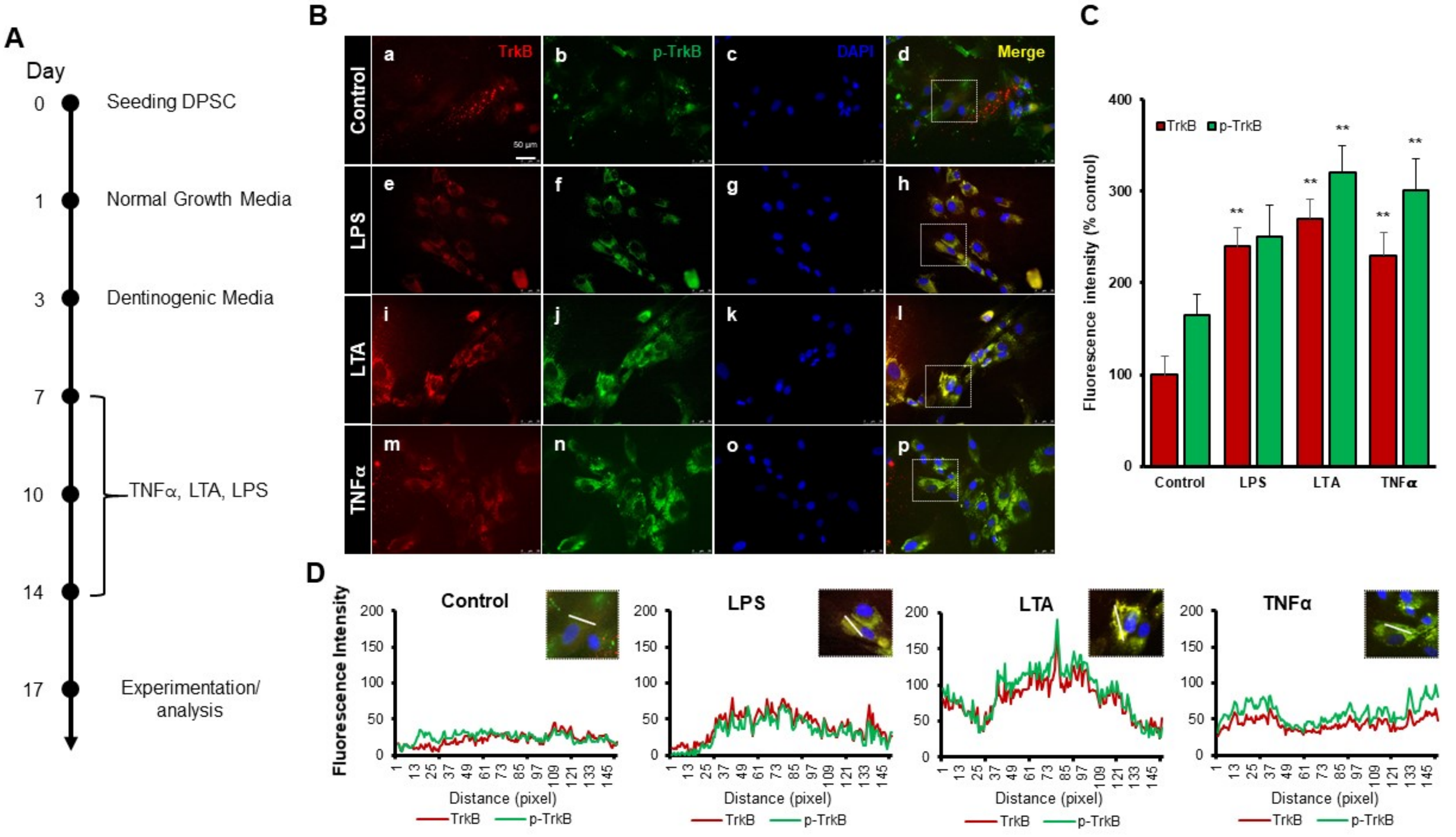
A
Day
0
Seeding DPSC
1
Normal Growth Media
3
Dentinogenic Media
7
10
14
TNFα, LTA, LPS
17
Experimentation/ analysis
B
Control
LPS
LTA
TNFα
a TrkB
b p-TrkB
c DAPI
d Merge
50 µm
C
TrkB
p-TrkB
Fluorescence intensity (% control)
400
300
200
100
0
**
Control
LPS
LTA
TNFα
D
Control
LPS
LTA
TNFα
Fluorescence Intensity
200
150
100
50
0
1 13 25 37 49 61 73 85 97 109 121 133 145
Distance (pixel)
TrkB
p-TrkB

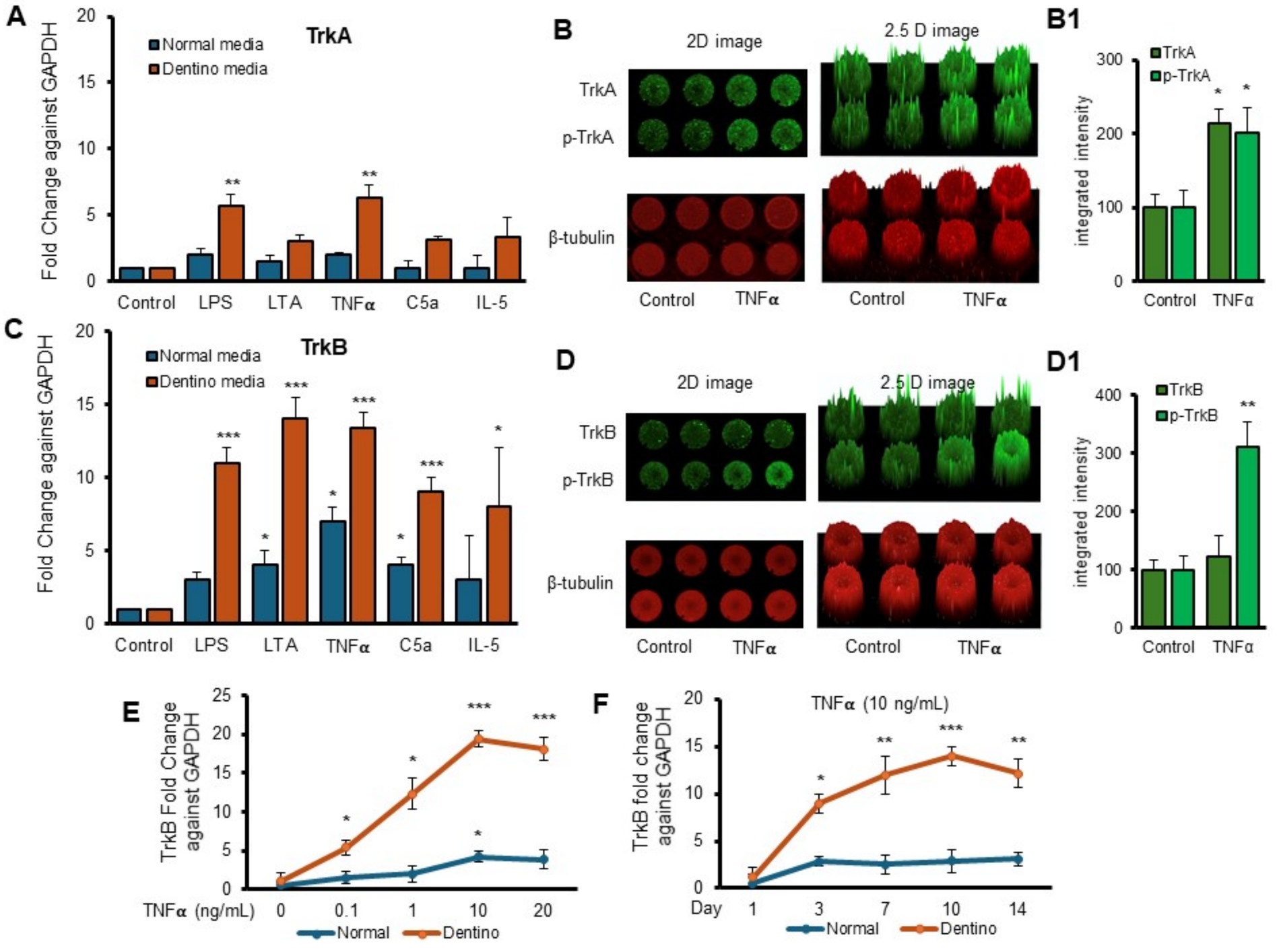
A
TrkA
Normal media
Dentino media
Fold Change against GAPDH
Control
LPS
LTA
TNFα
C5a
IL-5
B
2D image
2.5 D image
TrkA
p-TrkA
β-tubulin
Control
TNFα
B1
TrkA
p-TrkA
integrated intensity
C
TrkB
Normal media
Dentino media
Fold Change against GAPDH
D
2D image
2.5 D image
TrkB
p-TrkB
β-tubulin
D1
TrkB
p-TrkB
integrated intensity
E
TrkB Fold Change against GAPDH
TNFα (ng/mL)
Normal
Dentino
F
TNFα (10 ng/mL)
TrkB fold change against GAPDH
Day
Normal
Dentino

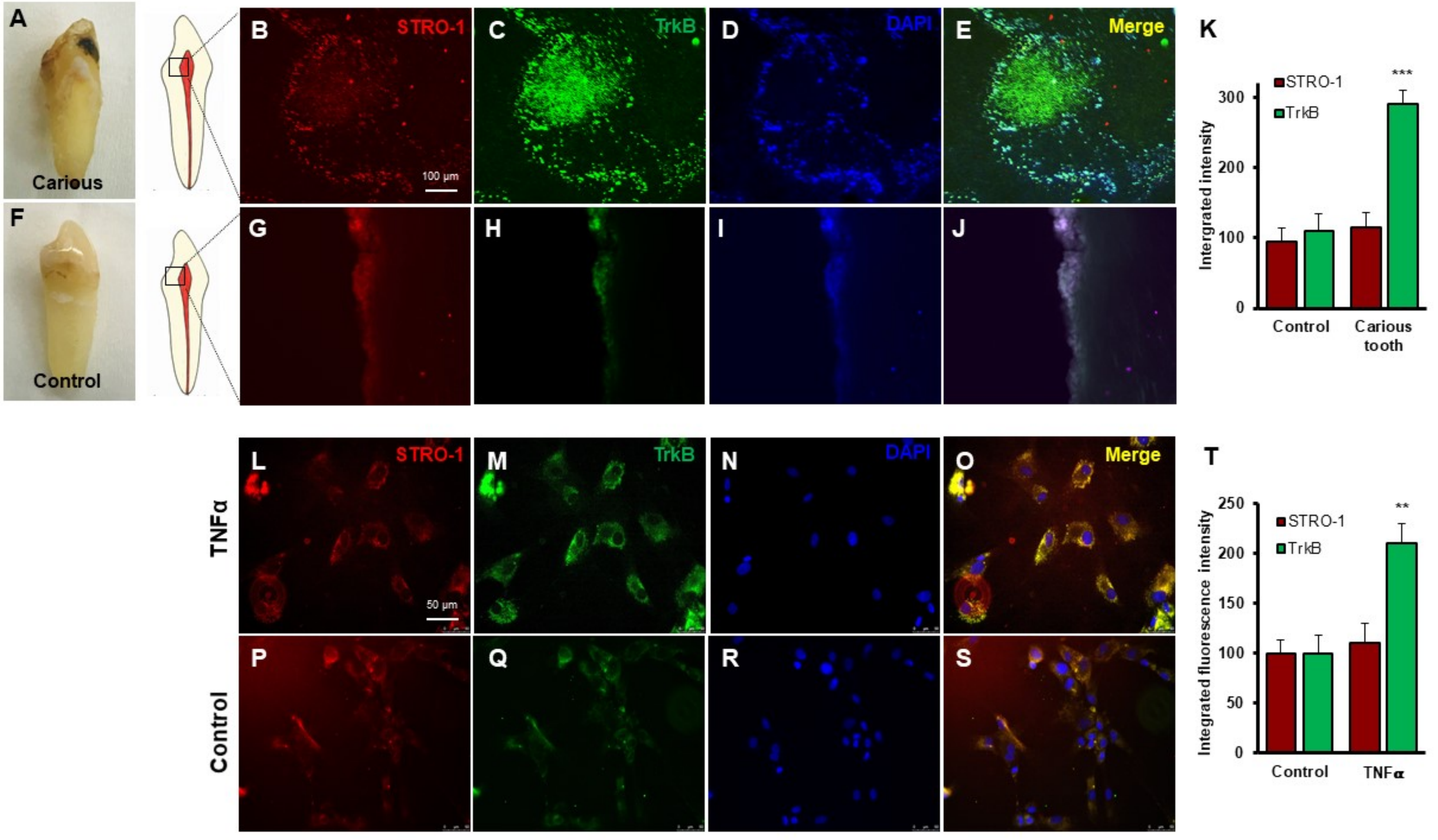
A
Carious
F
Control
B
STRO-1
100 μm
C
TrkB
D
DAPI
E
Merge
G
H
I
J
K
STRO-1
TrkB
***
Intergrated intensity
300
200
100
0
Control
Carious tooth
L
STRO-1
50 μm
M
TrkB
N
DAPI
O
Merge
TNFα
P
Q
R
S
Control
T
STRO-1
TrkB
**
Integrated fluorescence intensity
250
200
150
100
50
0
Control
TNFα

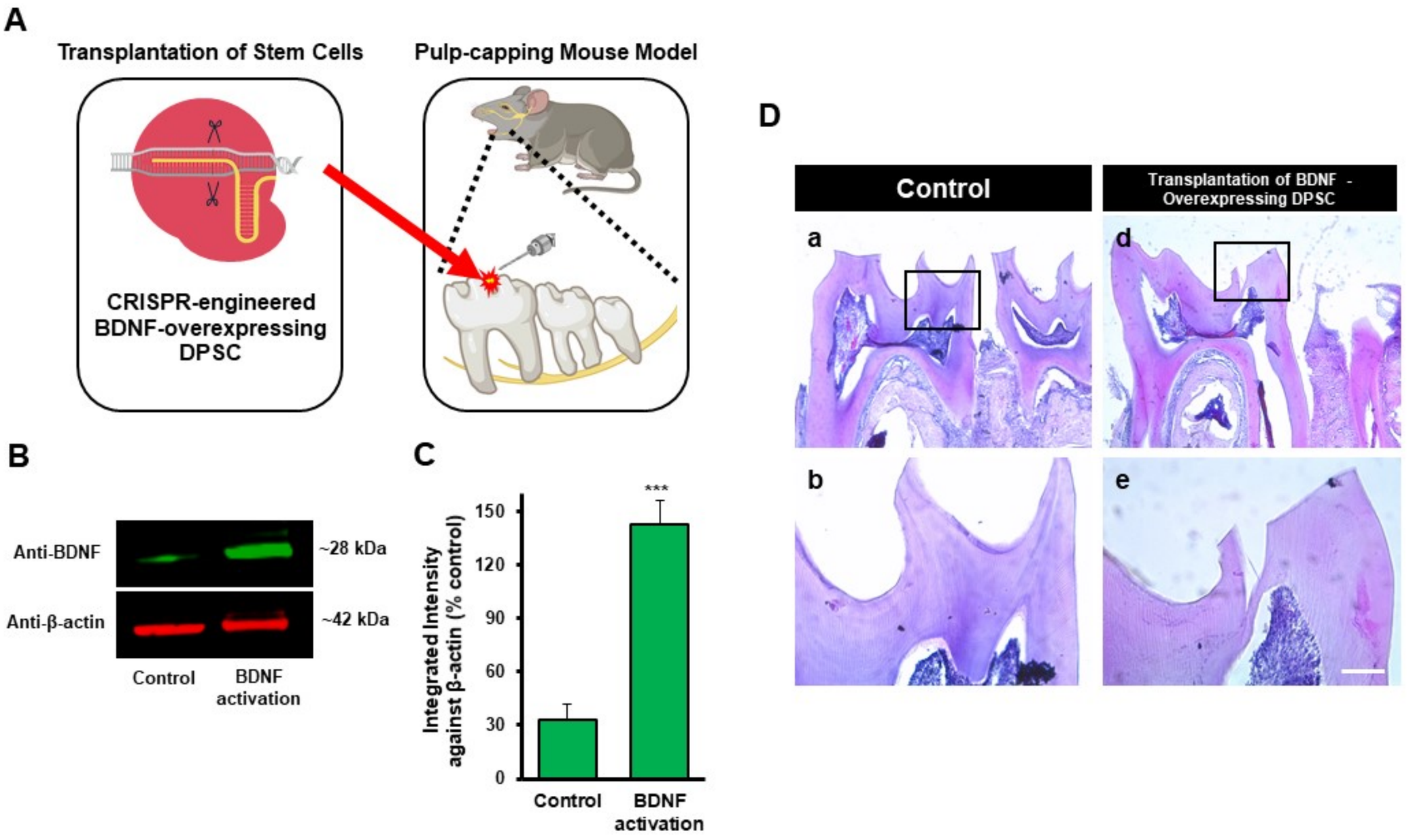
A
Transplantation of Stem Cells
Pulp-capping Mouse Model
CRISPR-engineered
BDNF-overexpressing
DPSC
B
Anti-BDNF
~28 kDa
Anti-β-actin
~42 kDa
Control
BDNF
activation
C
***
Integrated Intensity
against β-actin (% control)
150
120
90
60
30
0
Control
BDNF
activation
D
Control
Transplantation of BDNF -
Overexpressing DPSC
a
d
b
e

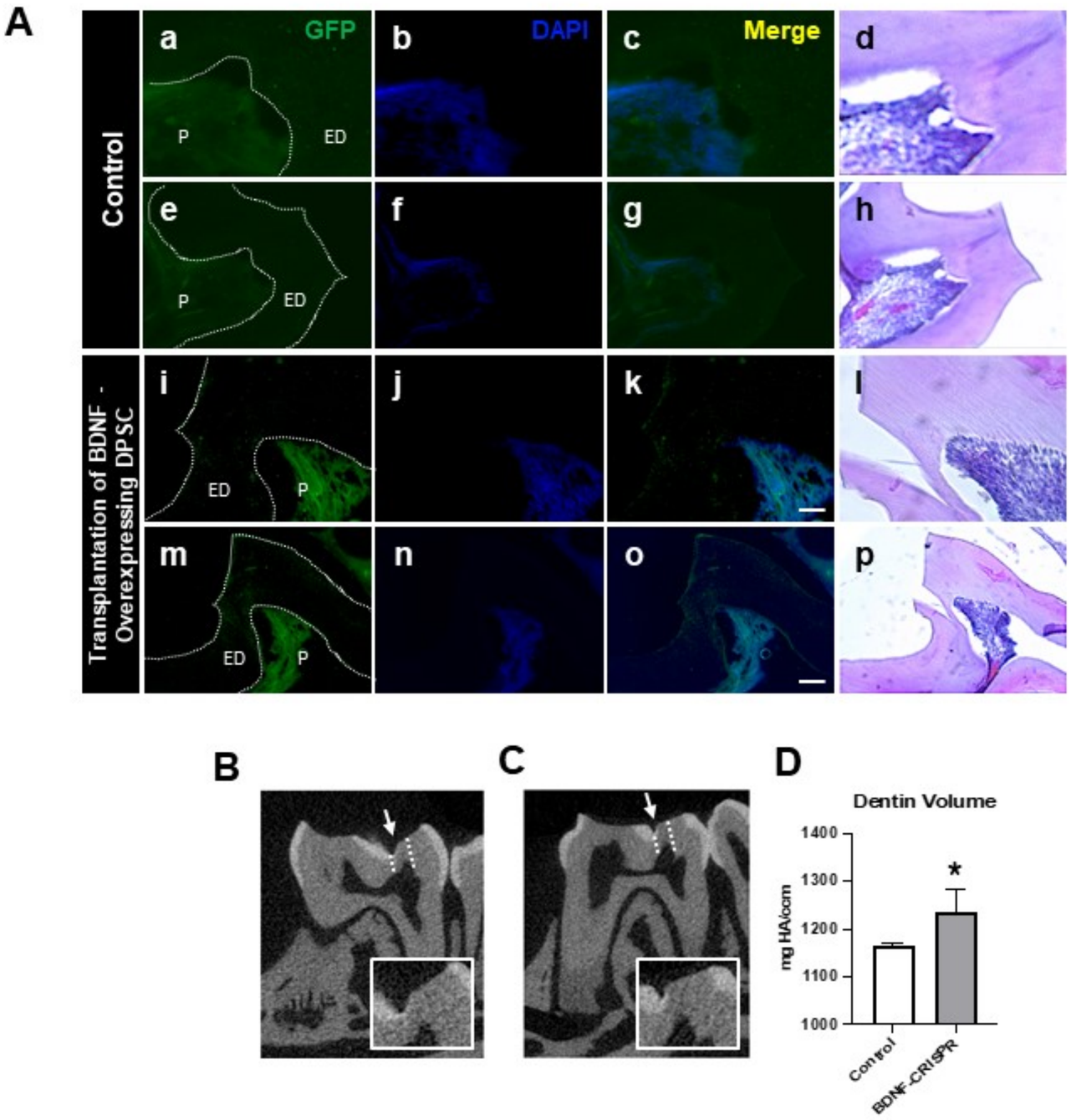
A
Control
Transplantation of BDNF - Overexpressing DPSC
a
GFP
b
DAPI
c
Merge
d
e
f
g
h
i
j
k
l
m
n
o
p
P
ED
B
C
D
Dentin Volume
mg HA/ccm
1400
1300
1200
1100
1000
*
Control
BDNF-CRISPR

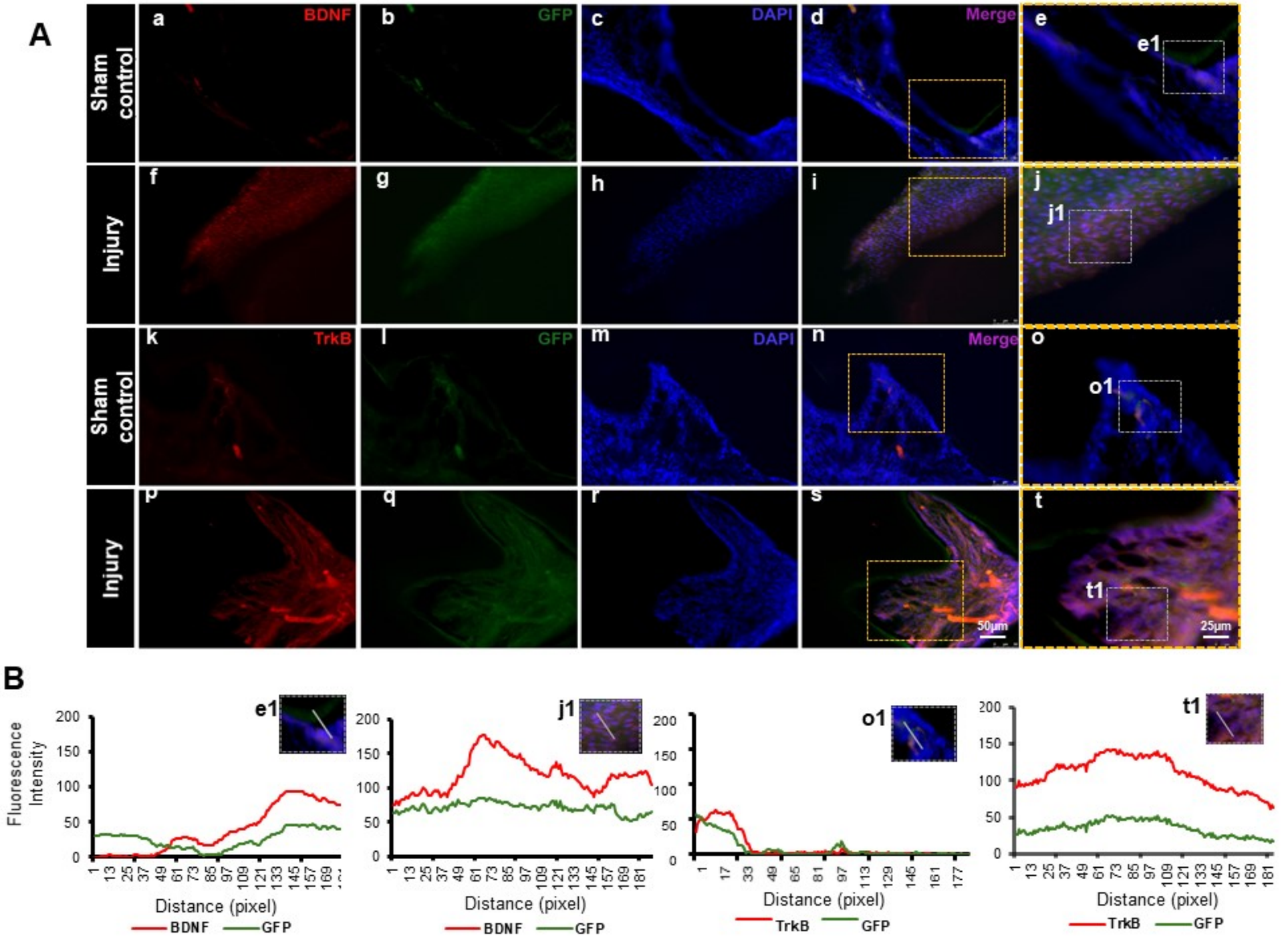
A
Sham control
Injury
Sham control
Injury
a
BDNF
b
GFP
c
DAPI
d
Merge
e
e1
f
g
h
i
j
j1
k
TrkB
l
GFP
m
DAPI
n
Merge
o
o1
p
q
r
s
t
t1
50μm
25μm
B
e1
j1
o1
t1
Fluorescence Intensity
Distance (pixel)
BDNF
GFP
TrkB
GFP

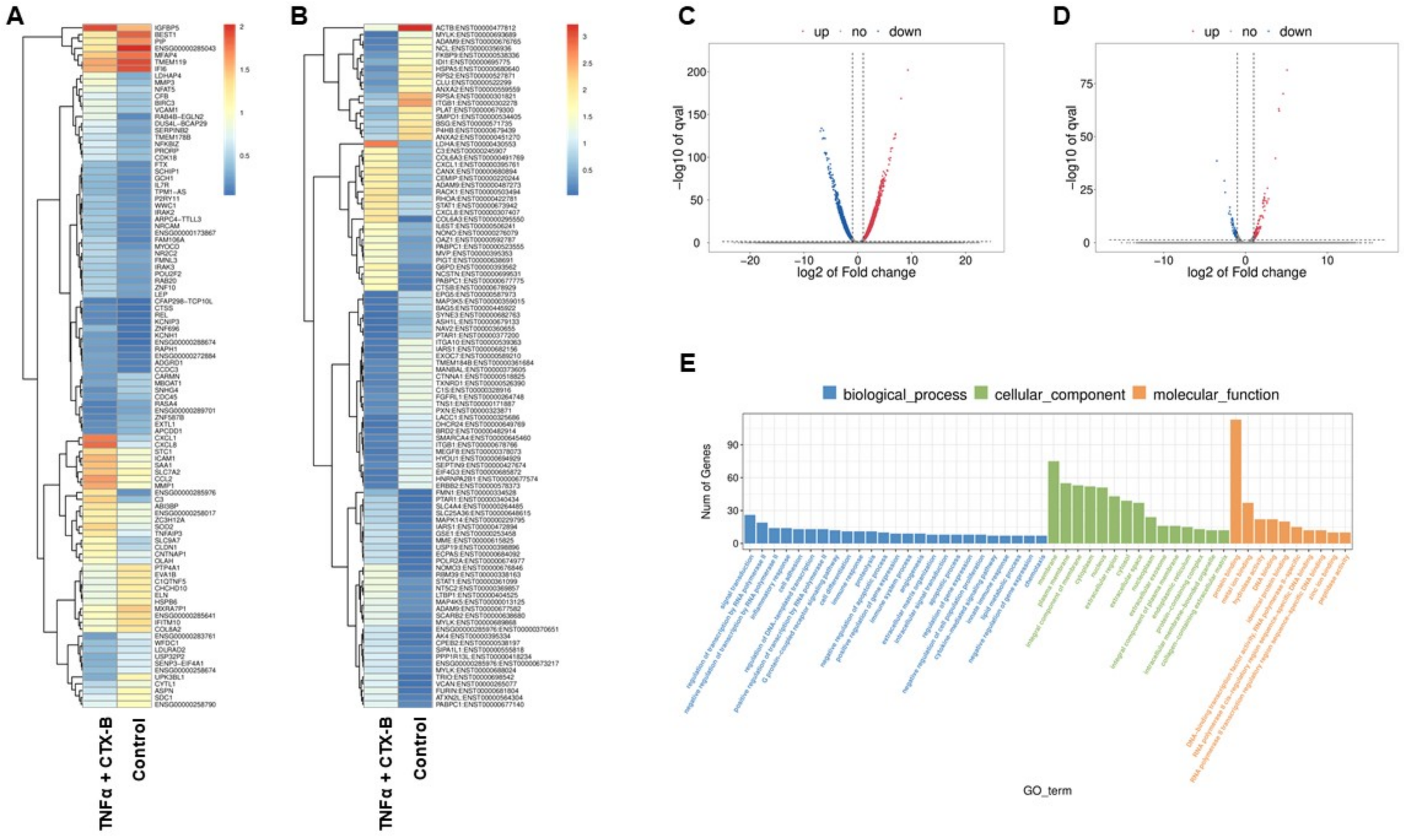
A
B
TNFα + CTX-B
Control
C
up
no
down
−log10 of qval
log2 of Fold change
D
up
no
down
−log10 of qval
log2 of Fold change
E
biological_process
cellular_component
molecular_function
Num of Genes
GO_term

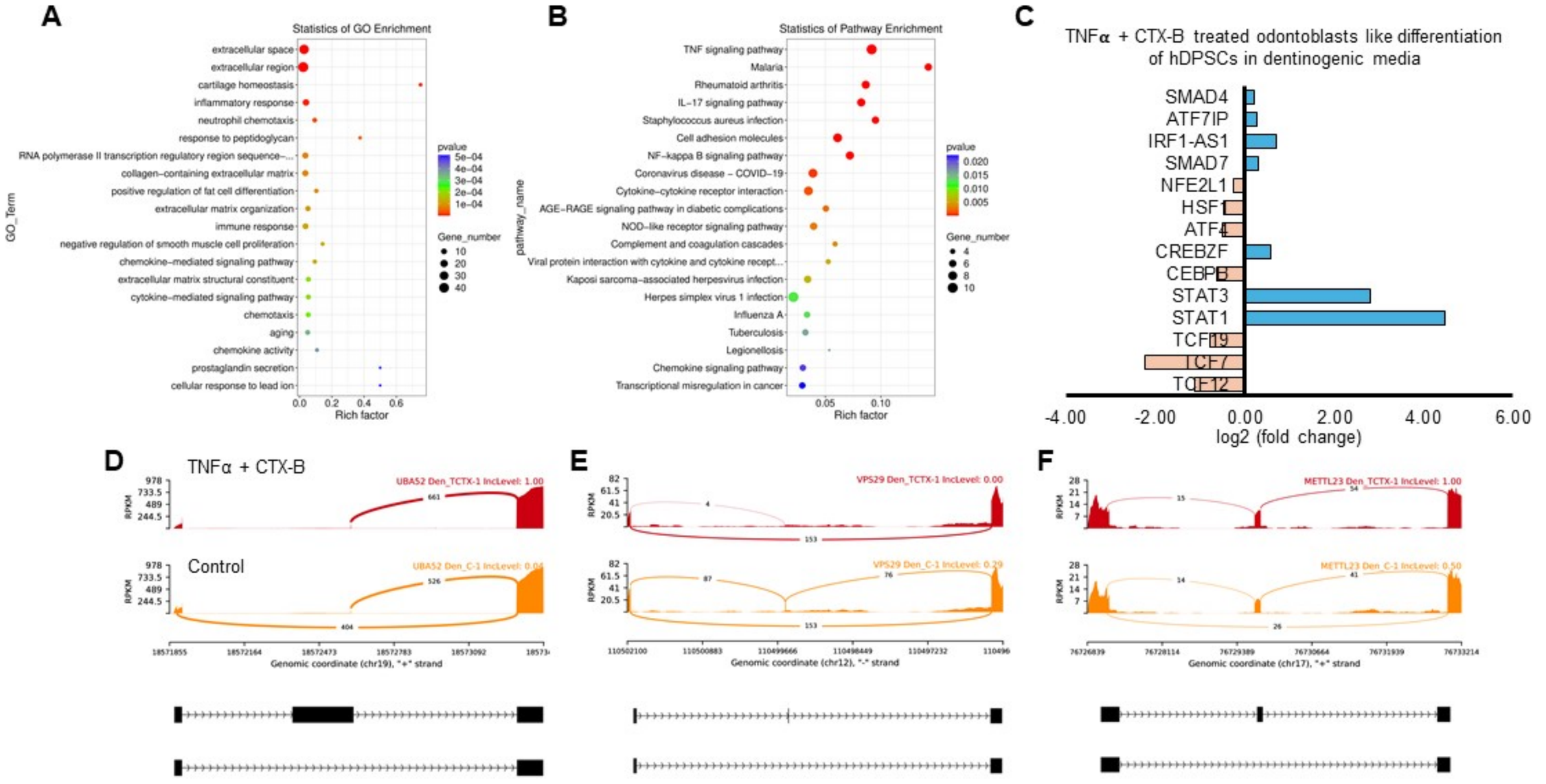
A
Statistics of GO Enrichment
extracellular space
extracellular region
cartilage homeostasis
inflammatory response
neutrophil chemotaxis
response to peptidoglycan
RNA polymerase II transcription regulatory region sequence-...
collagen-containing extracellular matrix
positive regulation of fat cell differentiation
extracellular matrix organization
immune response
negative regulation of smooth muscle cell proliferation
chemokine-mediated signaling pathway
extracellular matrix structural constituent
cytokine-mediated signaling pathway
chemotaxis
aging
chemokine activity
prostaglandin secretion
cellular response to lead ion
GO_Term
Rich factor
pvalue
Gene_number
B
Statistics of Pathway Enrichment
TNF signaling pathway
Malaria
Rheumatoid arthritis
IL-17 signaling pathway
Staphylococcus aureus infection
Cell adhesion molecules
NF-kappa B signaling pathway
Coronavirus disease - COVID-19
Cytokine-cytokine receptor interaction
AGE-RAGE signaling pathway in diabetic complications
NOD-like receptor signaling pathway
Complement and coagulation cascades
Viral protein interaction with cytokine and cytokine recept...
Kaposi sarcoma-associated herpesvirus infection
Herpes simplex virus 1 infection
Influenza A
Tuberculosis
Legionellosis
Chemokine signaling pathway
Transcriptional misregulation in cancer
pathway_name
Rich factor
pvalue
Gene_number
C
TNFα + CTX-B treated odontoblasts like differentiation of hDPSCs in dentinogenic media
SMAD4
ATF7IP
IRF1-AS1
SMAD7
NFE2L1
HSF1
ATF4
CREBZF
CEBPB
STAT3
STAT1
TCF19
TCF7
TCF12
log2 (fold change)
D
TNFα + CTX-B
Control
UBA52 Den_TCTX-1 IncLevel: 1.00
UBA52 Den_C-1 IncLevel: 0.04
RPKM
Genomic coordinate (chr19), "+" strand
E
VPS29 Den_TCTX-1 IncLevel: 0.00
VPS29 Den_C-1 IncLevel: 0.29
Genomic coordinate (chr12), "-" strand
F
METTL23 Den_TCTX-1 IncLevel: 1.00
METTL23 Den_C-1 IncLevel: 0.50
Genomic coordinate (chr17), "+" strand